

Stony Brook University



OFFICIAL COPY

The official electronic file of this thesis or dissertation is maintained by the University Libraries on behalf of The Graduate School at Stony Brook University.

© All Rights Reserved by Author.

Fabrication of High Performance Nanofiltration Membranes using Ionic Liquids

A Thesis Presented

by

Lewis Yung

to

the Graduate School

in Partial Fulfillment of the

Requirements

for the Degree of

Master of Science

In

Chemistry

Stony Brook University

August 2009

Stony Brook University

The Graduate School

Lewis Yung

We, the thesis committee for the above candidate for the
Master of Science degree, hereby recommend
acceptance of this thesis.

**Benjamin S. Hsiao – Thesis Advisor
Professor, Chemistry Department**

**Andreas Mayr – Chairperson of Defense
Professor, Chemistry Department**

**Robert B. Grubbs – Third Member
Professor, Chemistry Department**

This thesis is accepted by the Graduate School

Lawrence Martin
Dean of the Graduate School

Abstract of the Thesis

Fabrication of High Performance Nanofiltration Membranes using Ionic Liquids

by

Lewis Yung

Master of Science

In

Chemistry

Stony Brook University

2009

A new type of thin film nanofibrous composite membrane (TFNC) for nanofiltration (NF), prepared by interfacial polymerization (IP) of piperazine (PIP) using ionic liquids (IL) as additives and hexane as solvent, on electrospun polyethersulfone (PES) nanofibrous scaffold was demonstrated. A comparison was first made to illustrate the advantage of using highly porous electrospun nanofibrous PES scaffold versus typical ultrafiltration (UF) membrane as support for the PIP-based polyamide barrier layer. In fabricating the PES nanofibrous scaffold, a mixed solvent was used in electrospinning to improve the adhesion between the nanofiber and the polyethylene terephthalate (PET) non-woven substrate. During interfacial polymerization, two different ILs of different sizes were used: 1-octyl-3-methylimidazolium chloride (OMIC) and 1-butyl-3-methyl-imidazolium chloride (BMIC), to adjust permeate flux versus salt rejection (i.e., MgSO_4 and NaCl) properties; which were compared with those of commercial NF membranes (i.e. NF-90 and NF-270 from Dow FILMTEC). Results showed that TFNC prepared with electrospun nanofibrous scaffold exhibited significant better overall performance than conventional thin film composite (TFC)

membranes using UF membranes (i.e. PAN10 and PAN400) as scaffolds. The role of non-reactive IL exhibited a notable effect on improving the NF properties. The smaller ion (BMIC) simultaneously reduced permeate flux and increased salt rejection rate, while the larger ion (OMIC) exhibited an increase in permeate flux but a slight reduction in salt rejection. The best performing TFNC membranes exhibited comparatively high permeate flux and high divalent salt rejection performance as those of commercial NF membranes.

Table of Contents

List of Equations.....	vi
List of Figures.....	vii
List of Tables.....	viii
Acknowledgments.....	ix
1) Introduction.....	1
2) Experiment.....	5
2.1) Materials.....	5
2.2) Preparation of PES nanofibrous scaffold by electrospinning.....	5
2.3) Porosity measurement of the Electrospun nanofibrous scaffold.....	6
2.4) Fabrication of polyamide barrier layer by interfacial polymerization.....	6
2.5) Morphological Examination by Scanning Electron Microscopy.....	7
2.6) Salt Rejection Performance Evaluation.....	8
2.7) Molecular weight cut off (MWCO) test using aqueous of PEG.....	8
3) Results and Discussion.....	10
3.1) Comparison of DMF solvent versus DMF/ NMP mixed solvent for electrospinning Polyethersulfone nanofibers: adhesion, morphology, and fiber size distribution.....	10
3.2) Comparison of electrospun PES nanofibrous scaffold versus commercial UF membranes (PAN400 and PAN10) for interfacial polymerization of PIP and TMC.....	12
3.3) Effect of Ionic Liquid on permeation performance on NF membrane prepared by interfacial polymerization.....	15
3.4) Optimizing Formulation for improved filtration performance.....	24
4) Conclusion.....	30
References.....	33

List of Equations

Equation 1	6
Equation 2	8
Equation 3	8
Equation 4	9

List of Figures

Figure 1.....	11
Figure 2.....	12
Figure 3.....	13
Figure 4.....	17
Figure 5.....	18
Figure 6.....	19
Figure 7.....	22
Figure 8.....	24
Figure 9.....	26
Figure 10.....	26
Figure 11.....	28

List of Tables

Table 1.....	14
Table 2.....	23
Table 3.....	29

Acknowledgements:

Before you turn to the next page, I would like to say that I have never had a more fun and enlightening experience in an academic setting than I have had before entering Stony Brook University as an undergraduate. At Stony Brook University, I participated in their vast selection of events, made many friends, and more importantly I met many of the great faculty members across the campus. They have all given me inspirational and invaluable advices that I will cherish for the rest of my life.

My deepest gratitude and respect goes to my two thesis advisors, Professor Benjamin S. Hsiao and Professor Benjamin Chu, who have provided me with an amount of unconditional encouragement, invaluable advices, continuous patience, and much needed motivation while I was the way for my B.S. and M.S. Degree. They were more than just research advisors. They were also friends who offered important lessons on life and they guided me through times of frustration, whether it is in the lab or at home. Their support was always there.

I would also like to express my appreciation of the other members of my committee, Professor Robert B. Grubbs and Professor Andreas Mayr for their encouragement and suggestions during my studies to obtain an Master degree in Chemistry. I would like to thank all of my group members for giving me a very pleasant graduate experience. I would not have arrived this far without them.

Introduction:

Water is commonly found in large bodies, such as oceans, lakes, and streams. It can also be found in lesser quantities below ground level in aquifers or in the air as vapor. This ubiquitous substance totals to about 71% on the earth surface, yet only a very small fraction of it is being used for human consumption. The average human being is made of more than 50% of water alone and is constantly seeking ways to replenish this amount. The demands for quality water have become a very critical issue as the human population increases. One of the many innovations that have arisen to appease this dilemma is membrane filtration, which is one of the most affordable and efficient methods in purifying water [1].

Over the years, the advances on water filtration have given a very substantial control over water purification, which have enabled us to filter nearly all of the unwanted substances in water. Desalinating water is one of the most difficult processes in water filtration technology because it requires very precise control to effectively remove salt ions. Reverse osmosis (RO) membranes are engineered to produce freshwater from a saline source by rejecting all salt ions, while nanofiltration (NF) is a membrane process that filters nearly as many of the contaminations that are commonly found in easily obtainable water from faucets or nearby lakes [2]. NF is a pressure-driven membrane process that lies between ultrafiltration (UF) [3,4] and reverse osmosis (RO) [5]. The strength of NF system lies in its ability to retain substances with size greater than 1 nm in diameter [6,7] and charged ions [8], including amino acids, peptides and antibiotics. It is commonly used for water softening, removal of color, taste, odors and other small contaminates [9].

There are two main types of NF membranes that are commercially available: asymmetric membranes and thin film composite (TFC) membranes. The latter has proven to

be the more effective, exhibiting high flux and high salt rejection due to the presence of a nanoscale thin selective layer on the surface of the porous membrane. The key advantage of TFC membranes in comparison to the asymmetric approach is that each individual layer of a composite membrane can be optimized for its particular function, i.e. the thin barrier layer can be optimized for the desired solute rejection, while the porous substrate can be optimized for mechanical strength with minimum resistance to permeate flow. There are various methods employed to prepare TFC membranes, such as coating, plasma polymerization, and surface grafting [10].

Many NF membranes employ interfacial polymerized polyamide thin film as the barrier layer on top of a porous support (typically a UF membrane) [11,12,13]. However, recent studies have shown that the more porous support membrane could also play an effective role in increasing the permeate flux while maintaining high salt rejection (> 97%) [11,14]. Interfacial polymerization (IP) is a common method in creating a thin barrier layer for NF and RO applications [12,13,15]. The advantage of this method is its ability to fabricate an ultra-thin layer of highly cross-linked polymers between two insoluble phases (e.g., water and oil). Various parameters in the IP process (e.g. the reactant concentration, the type of additives, and the overall kinetics and diffusion rate of the reactants) as well as processing procedures (e.g. the reaction time, by-products removal, and pre and post treatments of the support scaffold) determine the performance of TFC membranes [2,9].

Recent studies have demonstrated the use of nanofibrous scaffolds as alternative scaffolds for TFC water filtration membranes [3,10]. Electrospinning is a process that can produce fine and continuous polymer nanofibers with submicron-sized diameters (1-3), varied porosity (25%-80%), and a large pore size range (2.7-0.17 μm) [3] thus making it a

susceptible component in the separation membrane for many filtration purposes [14]. Nanofibers have been used in applications, such as high performance air filters, tissue engineering, and removal of a great range of water contaminants [16,17,18,19]. In the electrospinning process, when a sufficiently high voltage is applied to a liquid droplet, the droplet becomes charged and begins to stretch. At a critical point, the body of the droplet counteracts with the surface tension and a stream of polymer fiber is formed after solvent evaporation. For fibers electrospun from polymer solutions, the presence of residual solvent in the electrospun fibers could induce bonding of intersecting fibers, creating a strong cohesive interconnected porous structure. The non-woven nanofibers can assemble into web-like network that exhibit good tensile strength and are extremely lightweight [20]. Polyethersulfone (PES) was chosen as the material for fabrication of nanofibrous scaffold by electrospinning because of its chemical inertness. Many of the commercially prepared TFC membranes are prepared by IP onto the surface of PES UF membranes. Previous works have shown the advantage of using an electrospun scaffold as support over conventional ultrafiltration membranes. Some of the characteristics of PES that make it suitable for water filtration are its high temperature resistance, great impact resistance, and good water absorption. In addition, PES is a relatively inexpensive material and remains in satisfactory condition over long-term continuous use without causing any dimensional change or physical deterioration [21].

In this study, a novel class of high flux TFC nanofibrous membrane formulated by using a high porosity PES nanofibrous scaffold electrospun onto a poly(ethylene terephthalate) (PET) non-woven substrate is used as the support for a ultra-thin layer of highly cross-linked amine monomers formed by interfacial polymerization. This ultra thin

layer serves as a selective barrier that is used to reduce the permeability of divalent salts (MgSO_4) and to retain substances with ~ 300 g/mol or greater [22]. The water flux and the salt rejection of the TFC membrane are mainly dependent on the chemical attribute of the selected monomers (i.e. hydrophilicity and molecular structure) and the thickness (i.e. the thinner the layer, the higher the permeation according to D'arcy's law) of the coating layer. Another method that would allow a higher permeability is to introduce water channels into the selective top layer. Previous studies have shown that by adding nanoparticles to the selective layer, an effective improvement on water permeability can also be achieved while maintaining a high degree of rejection. In this experiment, hexane was used to prepare the organic phase and two kinds of ionic liquid (IL) were used as the additive in the aqueous phase for the IP process. IL is an environmentally benign solvent that has been previously studied in other IP processes as a substitute to organic solvents [23,24]. In this case, the role of IL can range between the surfactant and the ionic salt to vary the nature of the aqueous phase for interfacial polymerization. Some of the characteristics that were expected by using IL in IP for fabricating the barrier layer of TFC membranes were simultaneous improvement in the membranes' permeate flux and in salt rejection.

2. Experiment

2.1 Materials

1,3,5 – benzenetricarbonyl trichloride (TMC), piperazine (PIP), triethylamine (TEA), magnesium sulfate heptahydrate ($\text{MgSO}_4 \cdot (\text{H}_2\text{O})_7$), dimethylformamide (DMF), and N-methyl-2-pyrrolidone (NMP), Polyethylene glycol (PEG) ($M_w = 400\text{g/mol}$ and 600g/mol) were purchased directly from Sigma-Aldrich. 1-octyl-3-methylimidazolium chloride (OMIC) was purchased from Acros Organic. 1-butyl-3-methyl-imidazolium chloride (BMIC) and PEG ($M_w = 200\text{ g/mol}$) were purchased from Fluka. NF-90 and NF-270 NF membrane were supplied by Dow Filmtec. PAN-400 and PAN-10 UF membrane were provided by Sepro Inc. (CA). Poly(ethylene terephthalate) (PET) non-woven substrate (PET Sanko 16-1 with an average fiber diameter of about $40\ \mu\text{m}$) used for the membrane support was purchased from Sanko Junyaku Co., Ltd. (Japan). Polyethersulfone (PES) powder ($M_w = 79,000\text{ g/mol}$) was purchased from Solvay S.A. (Belgium). 95% ethanol was purchased from Pharmco-Aaper (CT). All chemicals were used as received unless noted.

2.2 Preparation of PES nanofibrous scaffold by electrospinning

PES solution was prepared by dissolving PES in the mixed DMF/NMP solvent with ratios ranging from 2:8 to 8:2 (w/w) at $90\text{ }^\circ\text{C}$. The solution was stirred constantly with a mechanical stirrer for 2 days until it became homogenous. The electrospinning apparatus consisted of a grounded rotating metal collector, a syringe pump used to deliver PES solution through 4 spinnerets, and an oscillating stepping motor. A precut sheet of PET scaffold was mounted onto the grounded rotating collector. The PES solution was electrospun

simultaneously through the 4 spinnerets with diameters of 0.7 mm and at a distance 10 cm away from the collector. The applied voltage was 30 kV. To ensure the production of a uniform electrospun scaffold, a stepping motor was used to control the oscillatory translational motion perpendicular to the rotation direction of the collector. The distance traveled by the stepping motor was 18 cm. The PES solution flow rate for all 4 jets was 30 $\mu\text{l}/\text{min}$. A total of 2.4 ml of PES solution (0.6 ml/spinneret) was used to produce nanofiber scaffolds of thickness that ranged between 10-12 μm .

2.3. Porosity measurement of the Electrospun nanofibrous scaffold

The porosity of the electrospun membrane was determined by the following procedure. PES fibers were electro-spun directly onto PET. The PES nanofibrous layer was carefully removed and its density was measured. Its volume and weight was determined using a micrometer and a digital balance, respectively. The following equation was used to determine the porosity of the nanofibrous layer.

$$\text{Porosity} = \left(1 - \frac{\rho}{\rho_n}\right) \times 100 \quad (1)$$

ρ and ρ_n are the density of the electrospun substrate (by measuring the known size and dimension of the nanofibrous scaffold) and the bulk density ($\rho_n = 1.24 \text{ g}/\text{cm}^3$) of the PES powder, respectively.

2.4. Fabrication of polyamide barrier layer by interfacial polymerization

TFNC membranes were prepared by IP of PIP and TMC on electrospun PES nanofibrous scaffold and commercial UF membrane (i.e. PAN-10 and PAN-400). The

aqueous phase was prepared by dissolving an equal ratio of PIP and TEA (i.e. 0.125 - 1% (w/v)) in either water or ionic liquid. TEA was added to neutralize the acid formed after the polymerization. The organic phase was prepared by dissolving 0.1% (w/v) of TMC in hexane. Both solutions were stirred constantly with a magnetic stirring bar for 1 hr at room temperature before use. A precut sheet of PES electrospun nanofibrous scaffold and UF membranes (approximately 11 in. x 9 in. each) were used as the support layers for IP. To increase the hydrophilicity, these support layers were first soaked in ethanol and then rinsed with distilled water for several minutes. They were dried vertically for 1 min and then immersed in the aqueous amine solution for 4 min. The wet support layers were then placed on the surface of a smooth piece of glass. A rubber roller was gently rolled across their surfaces to remove the excess amine until there were no traces of water droplets visible. A dead weight was used to seal the edges of the amine-impregnated support layers and 60 ml of TMC solution was subsequently introduced to cover the entire surface for 1 min. After polymerization, the excess TMC solution was decanted and the TFNC membranes were allowed to dry vertically for 10 minute before washing with distilled water for 2 hrs to remove all the by-products. The membranes were stored in distilled water before further tests.

2.5. Morphological Examination by Scanning Electron Microscopy

The morphology of the electrospun PES nanofibrous support, UF and NF membranes, and TFC membranes were investigated by scanning electron microscopy (SEM, LEO 1550) after depositing a layer of gold coating. All samples were prepared by fracturing the sample in liquid nitrogen prior to gold coating.

2.6. Salt Rejection Performance Evaluation

A custom-built cross-flow water filtration evaluation system was used to measure the performance of the TFNC membranes. The system consisted of a tank for storing the brine, a water pump, a cooler, and 6 active cells, each with a working area of 42 cm². A 12 L brine was prepared by dissolving MgSO₄ or NaCl in distilled water to prepare the solution with a concentration of 2000 ppm. The brine was stored in the tank and the cooler was used to keep the temperature stable at 25 °C. All membranes were pre-compacted at 70 psi for 1 hr before any permeate was collected to limit the lateral movement of water during the performance test. The permeates were collected in plastic containers and the flux was measured according to the following equation.

$$Flux = (W_{total} - W_{container}) / t \quad (2)$$

W_{total} was the weight of the permeates and the container, $W_{container}$ was the weight of the container, and t was the time it took to collect the permeates. The salt rejection performances of the membranes were determined by measuring the permeate conductivity using a conductometer.

The percent rejection was determined according to the following equation.

$$rejection \% = (1 - \sigma_{permeate} / \sigma_{feed}) \times 100 \quad (3)$$

$\sigma_{permeate}$ was the permeate conductivity and σ_{feed} was the conductivity of the feed.

2.7. Molecular Weight Cut Off (MWCO) Test using Aqueous PEG Solution

The MWCO performance of the membranes was evaluated with 3 different feed

aqueous solutions containing 1000 ppm PEG with different molecular weights 200 g/mol, 400 g/mol, and 600 g/mol. A dead end cell with an active area of 11.5cm² was used for this evaluation. The permeate was collected at 25 psi of nitrogen gas. The permeates and the feed solutions were analyzed using total organic carbon analyzer (TOC), Shimadzu TOC-5000. The rejection was determined according to the following equation.

$$rejection \% = \left(1 - C_{permeate} / C_{feed}\right) \times 100 \quad (4)$$

$C_{permeate}$ was the permeate concentration and C_{feed} was the concentration of the feed.

3. Results and Discussion

3.1. Comparison of DMF solvent versus DMF/NMP mixed solvent for electrospinning of polyethersulfone nanofibers: adhesion, morphology, and fiber size distribution

Several factors were taken into consideration when determining the electrospinning parameters for desirable nanofiber properties [25]. (1) To reduce the amount defects on the membrane that could lead to fouling and lower rejection, a uniform surface is desired. The diameter size of the nanofibers contributes to the uniformity of the surface. (i.e. the smaller the diameter, the less coarse the surface would be) [26]. (2) The adhesion between the PES nanofibers and PET must be sufficiently good, thus strengthening the mechanical characteristics of the membrane. For (2), solvent mixtures of various concentration ratios of NMP and DMF were employed to control the evaporation rate of the solvent upon collection, thereby effectively controlling the adhesion between the PES nanofibers and the PET scaffold. A series of experiments using 22% (w/v) PES powder dissolved in different ratios of NMP/DMF (i.e. 2:8 to 8:2 (w/w)) mixed solvent were carried out to achieve fast and stable electrospinning conditions and to avoid compromising the quality of the PES nanofibers. The electrospinning conditions were operated with an applied voltage of 30 kV, with spinneret-to-collector distance of 10 cm, and a combined flow rate of 30 $\mu\text{l}/\text{min}$ for 4 jets. The temperature and the humidity were monitored such that the experiments were performed within the range of 23-25 $^{\circ}\text{C}$ and 20-30%, respectively. It was observed that by increasing the NMP/DMF ratio from 2:8 to 4:6(w/w), the strength of the adhesion between the forming PES nanofibrous layer and the PET scaffold increased. However, the evaporation rate of the solvent continued to decrease as the ratio of NMP/DMF increased from 4:6 to 8:2 (w/w). As

a consequence, there was no apparent fiber format because sufficient amount of solvent was retained upon collection. **Figure 1** shows SEM images of the surface of a PES substrate (22% (w/v) using PES with 4:6 (w/w) ratio of NMP/DMF) and PES substrate (22% (w/v) with PES in DMF). The surfaces of both nanofibrous scaffolds were produced by the random distribution of nanofibers, which resulted in a highly cross-linked network, with relatively random pores being extended throughout the scaffold. As observed, there were slight differences in the fiber diameter or ‘pore’ organization. Here the ‘pore’ geometry is somewhat ill-defined. One can probably consider an average pore size as the largest circular dimension of the opening. The frequency distribution of fiber diameter for the PES prepared by using the mix solvent in the electrospinning process is presented in **Figure 2**. The average fiber diameter was approximately 180 nm.

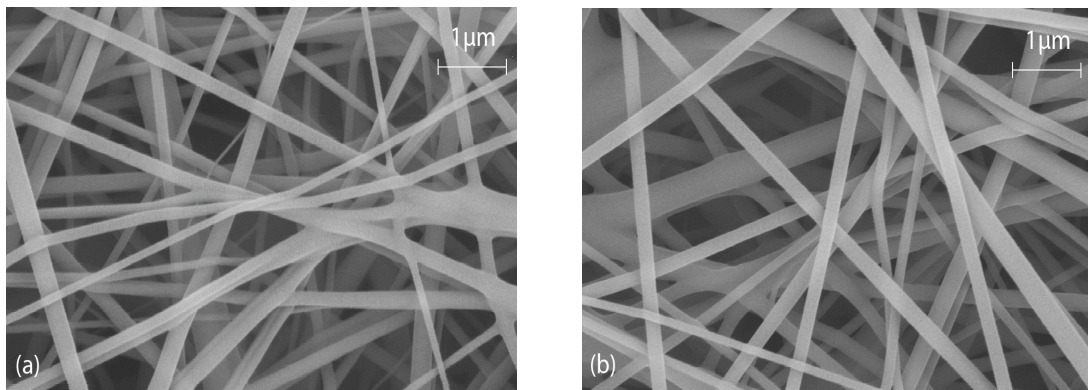


Figure 1 SEM surface images of (a) nanofibers based on 22%(w/v) PES in DMF, (b) nanofibers based on 22%(w/v) PES in NMP/DMF (4:6 (w/w)); all nanofibrous scaffolds were collected on a PET non-woven substrate.

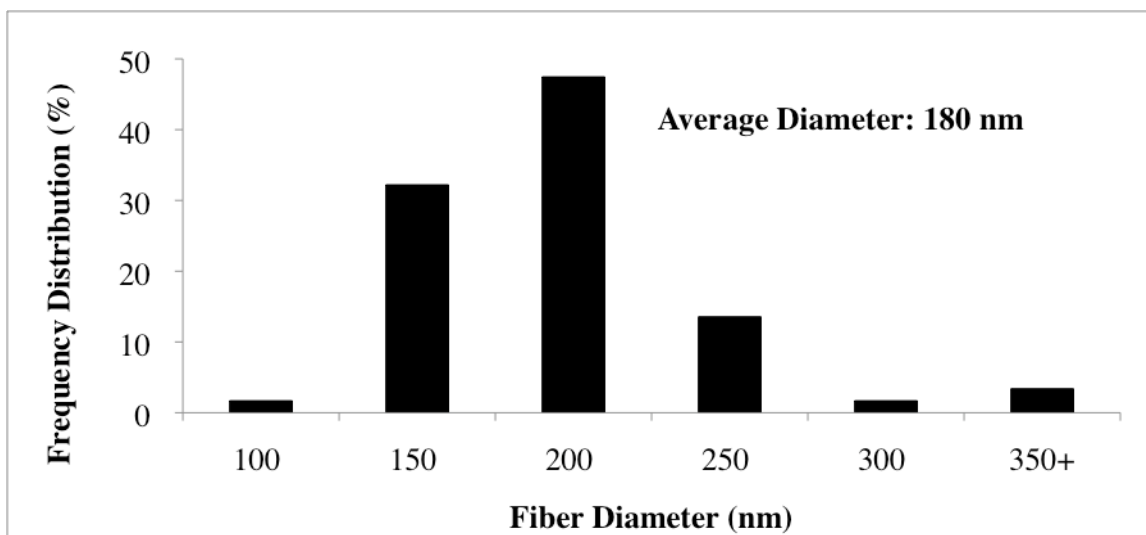


Figure 2 Diameter distribution of electrospun PES nanofiber using NMP/DMF (4:6 (w/w)) solvent.

3.2. Comparison of electrospun PES nanofibrous scaffold versus commercial UF membranes (PAN400 and PAN10) for interfacial polymerization of PIP and TMC

The active layers of conventional NF membranes have been fabricated by IP on UF membranes that exhibit relatively low permeate flux. **Figure 3** shows the surface morphology and the cross-section of two of the commercial UF membranes (PAN-10 and PAN-400) provided by Sepro Membranes. It was difficult to attain an accurate pore size distribution of these membranes base on the SEM images. Judging by the cross-section images of the UF membrane, it appears that they are composed of a thin uniform porous layer overlaid onto a dense fibrous scaffold. According to Sepro Membranes, the nominal marker (20K PEG) rejections for PAN-10 and PAN-400 were 95% and 75%, respectively [27]. The PES nanofibrous scaffold had an average fiber diameter of 180 nm and a porosity of about 84%. To demonstrate the advantage of using an electrospun scaffold in place of a conventional UF membrane, the same IP conditions (i.e. 1% (w/v) PIP in water with 0.1%

(w/v) TMC in hexane) were used to fabricate the PIP layer for all three of the support layers. The permeate behaviors were tested under cross-flow mode, using a feed solution of MgSO_4 at 2000 ppm and operating at 23.5-25 °C, and a pressure of 70 psi. **Table 1** lists the permeate flux and the percent rejection of the three membranes after an 1-hr test time.

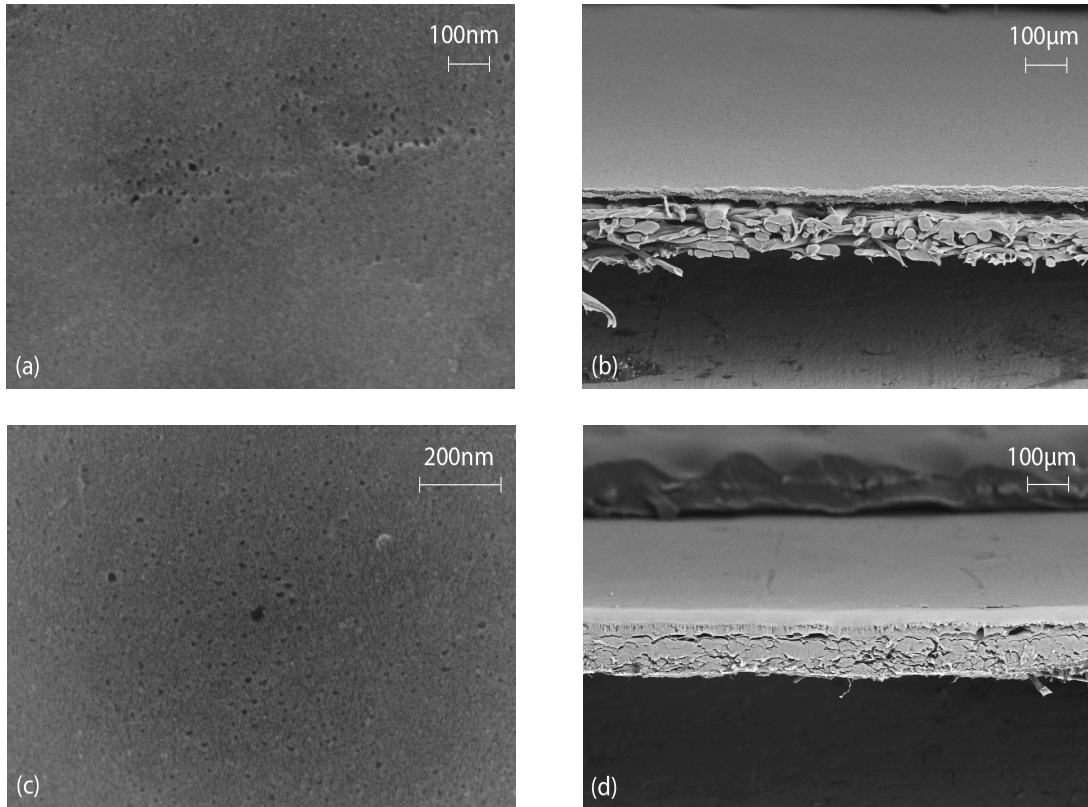


Figure 3 SEM images of the (a) surface of PAN400 (b) the cross-sectional view of PAN400 (c) the surface of PAN10 (d) the cross-sectional view of PAN10

TABLE 1 Water permeability and total MgSO₄ rejection for different types of nanofiltration systems

Barrier Layer / Scaffold	Flux (l/m²h)	Rejection (%)
1% PIP / electrospun PES on PET	32.45	99.1
1% PIP / PAN400	14.32	97.3
1% PIP / PAN10	12.99	85.5

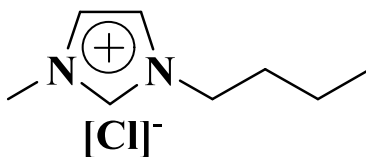
The TFNC membrane prepared by IP of 1% PIP on electrospun PES nanofibrous scaffold exhibited superior performance when compared with those prepared on the commercial UF membranes. The permeate flux of the TFNC membrane prepared on the PES nanofibrous scaffold was about 2.3 times of that of the TFNC membrane prepared with the PAN-400 UF membrane and about 2.5 times of that of the TFNC membrane prepared with the PAN-10 UF membrane. The higher permeate flux could be attributed to the greater porosity exhibited by the electrospun nanofibers scaffold than that of the UF membranes. The larger porosity of the electrospun PES nanofibrous scaffold has played a role in facilitating water passage through the membrane, resulting in a greater flux when compared with the TFNC membranes prepared by using UF membranes as substrates. The difference in flux between PAN-400 and PAN-10 also demonstrated a similar trend. The higher salt rejection of the TFC prepared on electrospun PES nanofibrous scaffold could also be partially attributed to the surface structure of the support, emphasizing the importance of the porous mid-layer support [28]. The pore density and pore size of the support could have served as reservoirs for PIP during the amine-soaking step of the IP process. Therefore by casting onto UF membranes, a less than expected amount of PIP actually participated in the polymerization process when compared with that of the electrospun PES nanofibrous scaffold, which had a greater pore density and a larger amine storage capacity. This

combination could result in a less dense and loose polyamide network formation and consequently, lower rejections for both TFC prepared with UF membranes. Although this study could imply that the process could be further adjusted by using a higher concentration of PIP to prepare the TFC, thereby increasing the membrane salt rejection rate, it is important to note that the corresponding change can lead to the build-up of a thicker polyamide layer that would increase the hydraulic resistance of the membrane and therefore decrease the permeate flux.

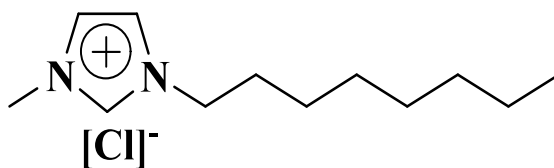
3.3. Effect of ionic liquid on permeation performance on NF membrane prepared by interfacial polymerization

Although research on room temperature ionic liquids is still relatively new, there have been reports that their use as solvents could lead to improvements in the rate and the yield of many organic syntheses and possibly including polymerization [29]. One group has used ionic liquids as solvents through the IP process [23]. In this study, the effects on the performance of TFC membranes using ILs (i.e, 1-butyl-3-methylimidazolium Chloride (BMIC) and 1-octyl-3-methylimidazolium Chloride (OMIC)) as solvents for PIP in the IP process were evaluated. **Figure 4** shows the chemical structures OMIC and BMIC. The ILs were first prepared by dissolving various concentrations of ions (i.e. 0.0-2.5% (w/v) BMIC or OMIC) in water and stirred with a magnetic stirring bar until they were homogeneous. 1%(w/v) PIP and 1% (w/v) TEA were subsequently added and stirred in the ILs for 1 hr. Thereafter, the same IP procedure described above was followed. Their effects on the polymerization of PIP were studied individually using the following cross flow filtration conditions: MgSO₄ at 2000 ppm and 70 psi. The total amine concentration was fixed at 1% (w/v) for all the membranes. **Figure 5** shows the TFC performance trend for membranes

prepared with OMIC and BMIC. The concentrations of the ions were systematically changed from 0.0-2.5% (w/v), while other parameters were fixed. The two different ILs produced contrasting results. The TFC membranes prepared with BMIC showed a decrease in flux from 32.45-12.86 l/m²h. Meanwhile the TFC membranes prepared with OMIC exhibited an increase in flux from 32.45-60.32 l/m²h. The MgSO₄ rejection for the TFC membranes prepared with BMIC increased slightly from 99.1% to 99.3% and the TFC membranes prepared with OMIC decreased from 99.1% to 91.9%. Overall, at 2.5% (w/v) ion concentration, the MgSO₄ rejection of the TFC membranes prepared with OMIC increased by 0.2% (or essentially remained unchanged) and was 8% greater than the TFC membranes prepared with OMIC. However, the permeate flux of the TFC membrane prepared with OMIC exhibited increases by 85% and 369% greater than the TFC membranes prepared with BMIC. This enormous increase could probably be attributed to the difference in the molecular size of the ions (BMIC: 174.67 g/mol; OMIC: 230.78 g/mol). Film casted on PAN400 membrane showed a similar behavior as well, [Figure 6](#).



(a) 1-butyl-3-methylimidazolium chloride ($C_8H_{15}ClN_2$)



(b) 1-octyl-3-methylimidazolium chloride ($C_{12}H_{23}ClN_2$)

Figure 4 Chemical formula of two chosen ionic liquids (a) 1-butyl-3-methylimidazolium chloride (BMIC) and (b) 1-octyl-3-methylimidazolium chloride (OMIC) . The size of these ions is proportional to the length of the side chain.

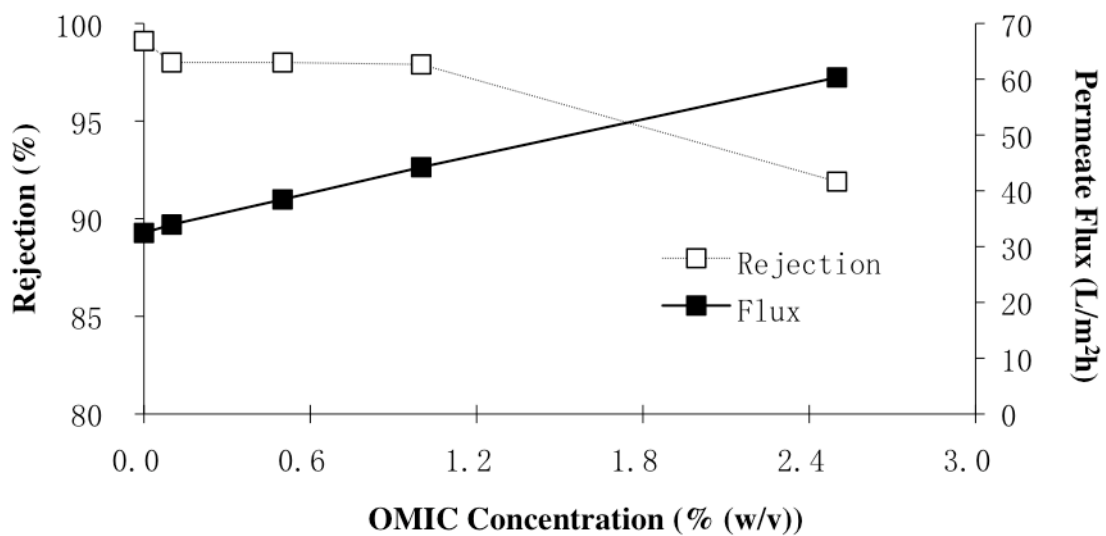
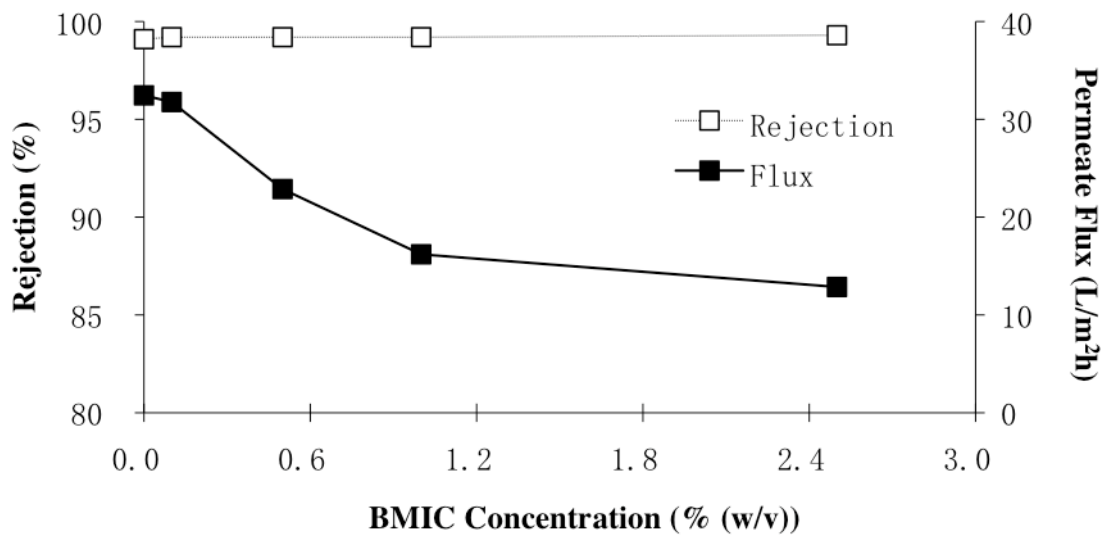


Figure 5 Dependence of magnesium sulfate (MgSO_4) rejection and permeate flux as a function of (a) BMIC concentration and (b) OMIC concentration for membrane prepared on electrospun PES nanofibrous scaffold (the permeate flux was evaluated with a cross flow filtration setup using 2000 ppm MgSO_4 at 70 psi)

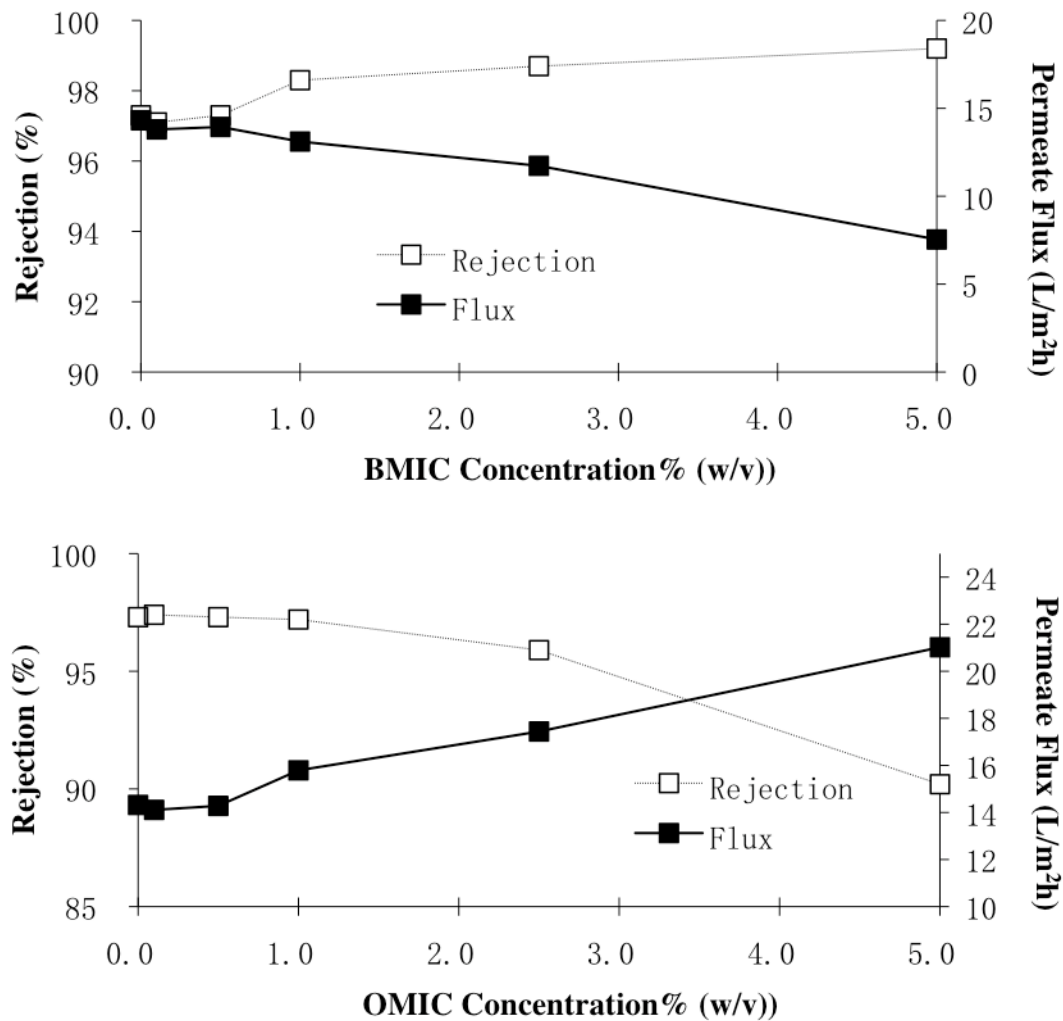


Figure 6 Dependence of magnesium sulfate (MgSO_4) rejection and permeate flux as a function of (a) BMIC concentration and (b) OMIC concentration for membrane prepared on PAN 400 (the permeate flux was evaluated with a cross flow filtration setup using 2000 ppm MgSO_4 at 70 psi)

There have been several reports of additive (e.g. surfactants, PEO, organic salts, and glycerol) used in the film casting solution to enhance the performance of the film during the formation of the interfacially polymerized polyamide network [30,31,32]. Their results indicated that these additives not only prevent the loss of porosity, but actively enhance the flux of the membrane [33]. The increase in the permeate flux and the slight decrease in the

divalent salt rejection by TFNC membranes prepared with OMIC suggest that OMIC may be carrying out a similar role to that of surfactants during the formation of the thin barrier layer. Like most surfactant, ionic liquids have a large polar head and a long hydrophobic tail in their structure. Therefore it is quite possible that they may behave in a very similar fashion. When OMIC was used as additives in the thin film formation, its hydrophobic structure were embedded into the polyamide lattice while the hydrophilic portion is freely exposed to water. As more OMIC accumulate within a region, the repulsion force between the hydrophilic polar heads and its neighbors increases. As a result, this increase the porosity of the film by enlarging the free volume within the polyamide matrix, thereby increasing the permeate flow and consequently the salt rejection diminishes. Another possibility may have had to do with the solubility of the ILs. According to R. Paterson the formation of the polyamide film is not exactly at the interface between the two phases but rather within and along the edge of the organic phase [2]. Therefore the solubility of OMIC in hexane is greater than the solubility of BMIC because of the longer carbon chain. This allows more OMIC to migrate toward the organic phase and thereby preventing the lattice from tightening.

On the contrary, the performance of membranes prepared with BMIC exhibits the opposite behavior; the permeate flux decreases and the salt rejection increased. One possibility for this difference in the membrane's performance that these two ionic liquid may serve a different roles during the formation of the film. Unlike OMIC, the length of the hydrophobic tail of BMIC is significantly shorter. The shorter aliphatic group of BMIC renders its behavior less like that of surfactants and more like a phase transfer catalyst. Like other phase transfer catalyst, it improves the rate of diffusion of the reactants across the interface and into the organic layer [34]. Others have shown that using ammonium ion

species as carrier to facilitate the transfer of reactants from the aqueous phase to the organic phase where the polymerization occurs [35]. These phase transfer catalyst function by ion pairing with the reactants and transferring it across the interface where the reactions occur [36,37]. Perhaps, because of its smaller dimension and greater force of attraction (due to its smaller ionic radius), BMIC behavior is similar to a phase transfer catalyst and it is able to readily absorb the PIP from the aqueous layer and transfer it to organic phase. Not only does improve the transfer mechanism across the interface but it also increases the diffusion rate. Consequently, a denser and thicker film is formed which rise to a higher rejection rate and higher resistance to permeate flow.

ATR was used to determine if IL resided within the PIP lattice after washing the TFNC membrane. **Figure 7** shows the infrared absorbance spectrum of OMIC, BMIC, PES nanofibrous scaffold, and TFNC membrane prepared by IP with ILs. The aliphatic group of BMIC and OMIC are represented by the very sharp peaks between 2850 to 3385 cm^{-1} region on their respective spectrum. While the broad feature at 3000 to 3500 cm^{-1} represents the imidazole group of the ILs. However, these two peaks do not appear in the spectrum of the PIP film which indicates that the ILs do not exist in the final product of the polymerization.

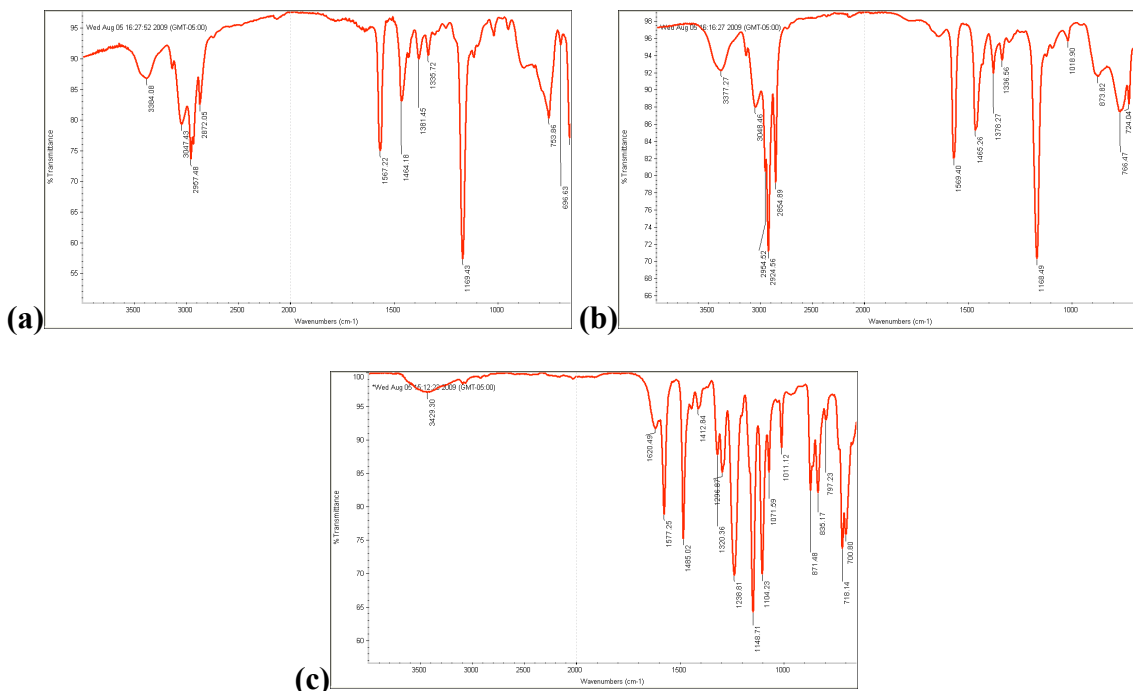


Figure 7 ATR spectra of (a) BMIC (b) OMIC and (c) TFNC membrane prepared with Ionic Liquid

Table 2 shows the MWCO of several TFNC membranes. Membranes prepared by IP with 1% BMIC demonstrated a highest rejection of all three Mw PEG tested compared with the other TFNC membranes. In contrast, membranes prepared with 1% OMIC demonstrated lower rejection. It is notable that for TFNC membrane prepared with 1% OMIC exhibit approximately 57.5% rejection for PEG – 400 and only 41.3% rejection for PEG-200. Comparing that to the molecular weight of OMIC (i.e. 230.78 g/mol), it is safe to assume that most, if not all, of the IL was removed during the wash after the polymerization step and the during the hour of pre-compacting the membrane before testing. Similarly, PEG-200 rejection for TFNC membrane prepared with 1% BMIC (molecular weight = 174.67g/mol) exhibited only 52.3% rejection, thus it is probable that it was successfully flushed out as well.

Table 2 MWCO of membranes prepared by interfacial polymerization on nanofibrous scaffold.

Membranes	PEG – 200	PEG - 400	PEG – 600
1% PIP	46.2 ± 6.7%	62.3 ± 1.6%	90.9 ± 4.3%
1% PIP BMIC 1%	52.3 ± 3.9%	74.2 ± 3.2%	92.3 ± 1.4%
1% PIP OMIC 1%	41.3 ± 1.2%	57.5 ± 6.0%	83.3 ± 4.3%

A comparison of the salt rejection (i.e. MgSO₄ and NaCl) between TFNC membranes prepared with ILs (i.e. OMIC and BMIC) and water as solvent for the IP of 1% PIP was made. Their performance was evaluated by using the following 2 conditions on a cross-flow filtration setup: MgSO₄ at 2000 ppm at 70 psi and NaCl at 2000 ppm at 70 psi. There could be a correlation between the molecular size of the ILs and the performance of the TFNC membranes due the different packing variation of PIP during the polymerization process. Divalent and monovalent salt rejection performance of the three TFNC membranes is illustrated in [Figure 8](#). During the NaCl rejection test, the rejection exhibited by the TFNC membrane prepared by BMIC was 58%, which is 55% greater than that prepared with water (37.3% NaCl rejection) and 138% greater than the TFNC membrane prepared with OMIC (24.3%), implying that BMIC could have tightened the lattice by accelerating the polymerization process, which resulted in a more densely packed amide chains. When the MgSO₄ rejection performances of the three TFC membranes were evaluated, all three TFNC membranes exhibited high salt rejection (>97%). As predicted, both of these membranes exhibited rejections that deviated in opposite directions from the TFNC membrane prepared without using IL. The TFNC membrane prepared with BMIC demonstrated the highest rejection at 99.2% and the TFNC membrane prepared with OMIC had the lowest salt rejection at 97.2%.

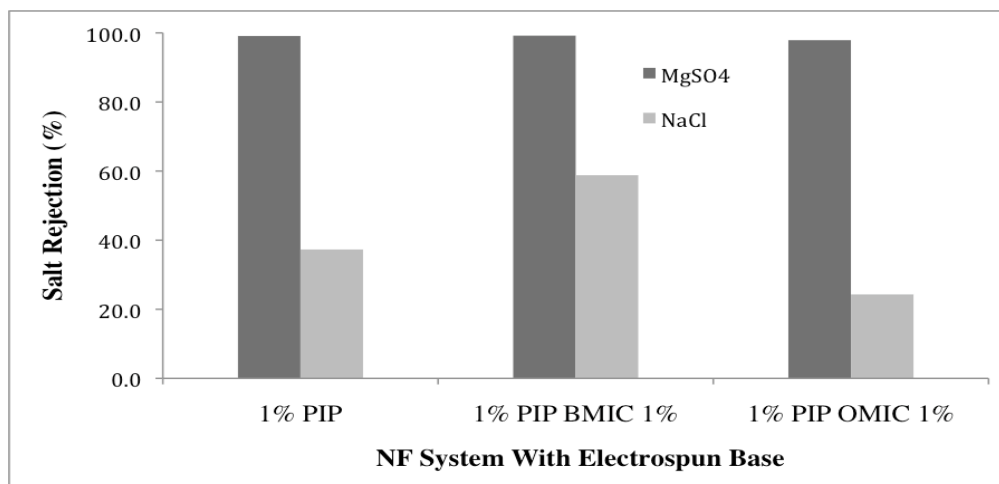


Figure 8 NaCl and MgSO₄ rejection for three kinds of TFNC membranes, each prepared using a different solvent for interfacial polymerization of 1% PIP (distilled water, 1% BMIC and 1% OMIC) evaluated with a cross flow filtration setup: 2000 ppm MgSO₄ at 70 psi.

By increasing the concentration of BMIC, the salt rejection for both MgSO₄ and NaCl improved, while the permeate flux drastically decreased. In contrast, an increase in the concentration of OMIC reduced the salt rejection, but improved the permeate flux. Overall, the results indicated that by selecting the IL and controlling its concentration used for IP, one could adjust the rejection and the permeate flux of the TFNC membranes accordingly.

3.4. Optimizing Formulation for improved filtration performance

The polyamide barrier layer is the most important component of the three layers to the membrane performance for size separation. Many modifications can be made to the top layer to improve the permeate flux of a TFNC membrane and at the same time, to maintain a respectable salt rejection (e.g., >90%). One method that was employed was by adjusting the PIP concentration. In this study, a set of concentrations of PIP (i.e. 0.125% to 1% (w/v)) was dissolved in water, while all other parameters for the polymerization were held constant. The performances of the TFNC membranes were evaluated using a cross-flow filtration system

with MgSO_4 at 2000 ppm and an operating pressure of 70 psi. **Figure 9** shows the relationship between the PIP concentration and the TFNC performance (i.e. permeate flux rate and salt rejection). As the PIP concentration was systematically decreased from 1% to 0.125% (w/v) the permeate flux was increased and the salt rejection was well maintained above 91%. The lowest PIP concentration (i.e. 0.125%) for the TFNC membrane demonstrated a high flux of $75.09 \text{ l/m}^2\text{h}$ with a 91.4% salt rejection and the highest PIP concentration (i.e. 1%) tested showed a lower permeation flux of $32.45 \text{ l/m}^2\text{h}$ with an even higher salt rejection at 97.1%. Overall, the results showed that the permeate flux increased by 131% and rejection decrease by 6% with the decrease in PIP concentration (1% to 0.125% (w/v)). It also appears that the greatest change in flux and rejection occurred at 0.25% (w/v) PIP (salt rejection: 97.7%, permeate flux: $44.28 \text{ l/m}^2\text{h}$). The increase in the permeate flux as the PIP concentration was decreased could be due to the change in the thickness of the polyamide layer. A SEM cross-section and surface of the TFNC membrane prepared with 1% (w/v) PIP is shown in **Figure 10**. It could be assumed that as the concentration of PIP was increased, the polyamide layer became thicker, thereby increasing the hydraulic resistance and reducing the permeate flux. This change has also led to a slightly higher salt rejection as the thicker top layer was also accompanied by an increase in the density of the polyamide chains.

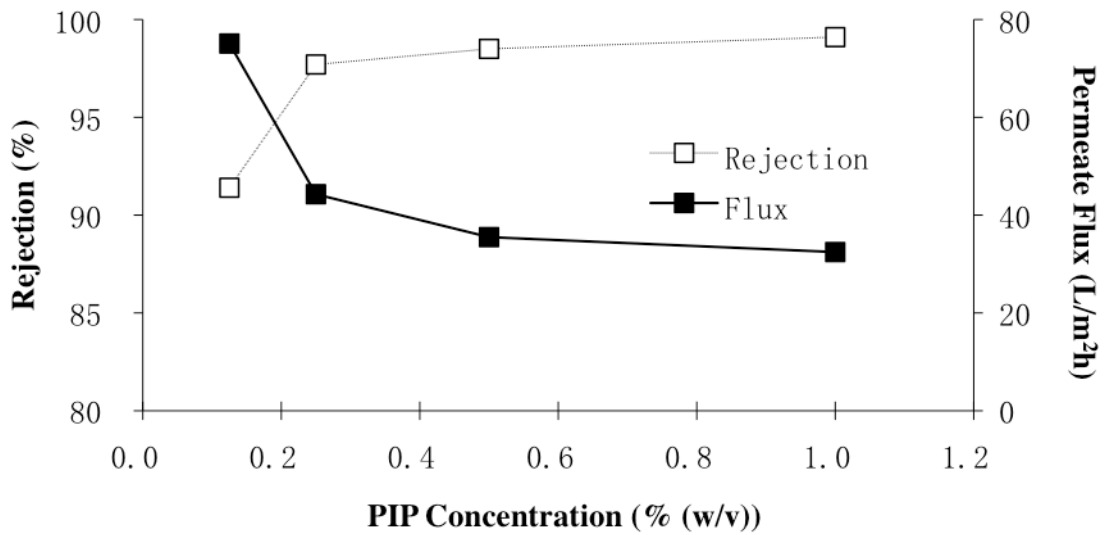


Figure 9 MgSO₄ rejection and permeate flux of TFNC as a function of PIP concentration (the NF properties were evaluated with a cross flow filtration setup: 2000 ppm MgSO₄ at 70 psi).

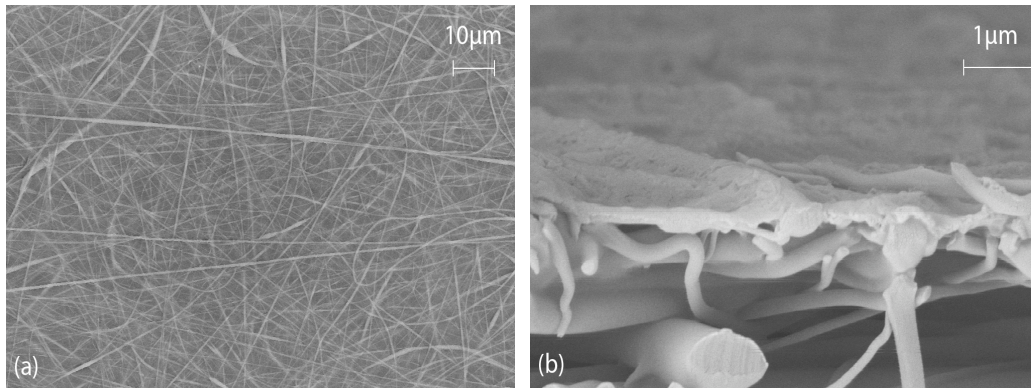


Figure 10 (a) Surface and (b) cross section image of TFNC membrane prepared by interfacial polymerization using 1% PIP (no IL was used).

Another variable that could be adjusted to improve the performance of the TFNC membranes was by varying the concentration of the IL. It was found previously that by fixing the concentration of PIP at 1% and by increasing the concentration of OMIC from 0.1 to 2.5% (w/v), the flux improved from 32.45 to 60.32 l/m²h while the MgSO₄ rejection rate

decreased slightly from 99.1 to 91.9%. In this experiment, the performance of the TFNC membrane of varying concentration of OMIC was reevaluated with a lower concentration of PIP (i.e. 0.5% (w/v)). **Figure 11** shows the relationship between the OMIC concentration, the permeate flux, and the rejection rate of TFNC membranes. When the OMIC concentration was increased from 0.0 to 0.5 % (w/v), the flux was increased from 35.50 to 70.23 l/m²h and the rejection rate decreased from 98.5 to 94.2%. Overall, the flux increased by 97.8% and the rejection decreased by 4.6%. Although the data is not shown, the TFNC membranes exhibited even greater permeate flux accompanied by a much steeper decrease in salt rejection with a further increase in the OMIC concentration, It also appears that the lower the concentration of PIP, the thinner the PIP barrier layer becomes. The TFNC membrane achieved a greater flux at a much lower concentration of OMIC with higher salt rejection. For instance, the TFNC membrane prepared with 1% PIP was able to achieve a permeate flux of 44.23 l/m²h and MgSO₄ rejection of 97.9% at 1% OMIC (w/v). Meanwhile, the TFNC membrane prepared with 0.5% PIP was able to achieve a similar performance at a much lower OMIC concentration, i.e., 0.05% (w/v) with a permeate flux of 46.43 l/m²h and a MgSO₄ rejection of 97.8%. This significant reduction in the amount of OMIC required to attain similar results strongly implied that that the thickness of the PIP barrier layer was an important factor in determining the amount of OMIC required to enhance the performance of the membrane. Moreover, better performance of the TFNC can be achieved with lesser amount of materials.

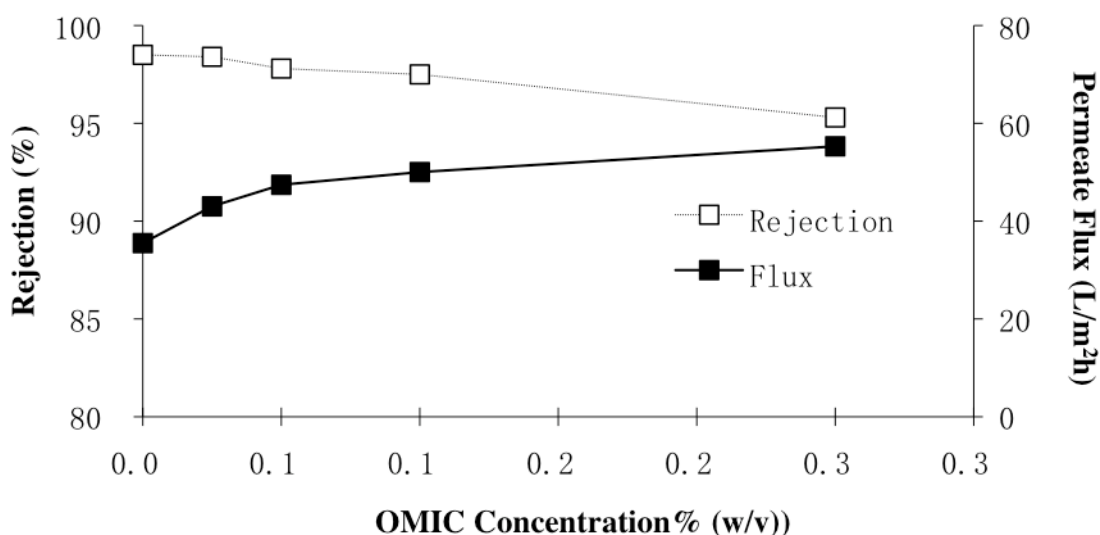


Figure 11 MgSO₄ rejection and permeate flux as a function of OMIC concentration evaluated with a cross flow filtration setup: 2000 ppm MgSO₄ at 70 psi.

Table 3 list the performance of TNFC membranes prepared by IP of PIP with and without OMIC on electrospun nanofibrous support and 2 commercial NF membranes (i.e. NF-90 and NF-270) were compared under the same cross-flow filtration settings: 2000 ppm MgSO₄ at 70psi. NF-90 and NF-270 are two membranes used for nanofiltration (i.e. separation of divalent salt) that are prepared by IP of piperazamide on polysulfone microporous support [11, 38]. These two commercial membrane NF-90 and NF-270 exhibited high salt rejection (>97%) and NF-270 permeate flux exceeded that of NF-90 by close to a factor of 2 (i.e. NF-270: 50.21 l/m²h and NF-90: 27.22 l/m²h). The TFC membrane that was optimized with 0.5% (w/v) PIP and 0.1% (w/v) OMIC exhibited close to identical values (i.e. (permeate flux: 50.03 l/m²h and salt rejection 97.8 %) of the high end commercial NF-270 and the flux was also twice as large as that of the more commonly available NF-90. In addition, the TFNC membrane prepared with water also resulted in higher flux (i.e. 35.5l/m²h) with similar salt rejection (i.e. 98.5%) when compared with the NF-90.

Table 3 Water Permeability and Total Salt Rejection For Different Types Of Nanofiltration systems

Barrier Layer / Scaffold	Flux (l/m²h)	Rejection (%)
.5% PIP / electrospun PES on PET	35.5	98.5
.5% PIP & .1% OMIC / electrospun PES on PET	50.0	97.8
NF-90	27.2	99.0
NF-270	50.2	97.4

4. Conclusions

The present study has been focused primarily on the effects of ionic liquids (i.e. OMIC and BMIC) as a solvent for interfacial polymerization of piperazine and trimesoyl chloride on electrospun PES nanofibrous scaffold. Prior to evaluating the ionic liquids as a viable solvent, the solvent consisting of a mixture of NMP and DMP (4:6 (wt/wt) ratio, respectively) was used to prepare the PES solution to enhance the adhesion between the nanofibers and the PET substrate during the electrospinning process. Electrospinning conditions were carefully adjusted to produce very fine fibers with an average fiber diameter of 180 nm, forming a uniform scaffold with little defects or bead formation. These new nanofibrous scaffolds were subsequently used as supports for a PIP polyamide barrier layer produced by interfacial polymerization. In addition, an experiment was conducted to demonstrate the advantages of using the electrospun nanofibrous scaffold as oppose to conventional UF membranes as supports for interfacial polymerization. The performance of those membranes was evaluated with a cross-flow filtration system using divalent salt (i.e., $MgSO_4$) at 70 psi. It was observed that the TFNC membrane prepared with PES nanofibrous scaffold exhibited a greater permeate flux and salt rejection under the same polymerization conditions (i.e. 1% (w/v) PIP and TEA of equal ratio with respect to PIP dissolved in water and 0.1% (w/v) TMC dissolved in hexane). This could be attributed to the large surface porosity and the greater pore density of the nanofibrous scaffold when compared with the microporous structure of UF membranes. Moreover, the decrease in rejection as seen in the UF membranes could be attributed to surface pores that might also serve as reservoirs to facilitate the mass transfer of reactants from the aqueous phase (i.e. water) to the organic phase (i.e. hexane), thereby mediating the thickness and the density of the polyamide barrier

layer during interfacial polymerization. Similar trend was also exhibited between the two UF membranes (i.e. PAN400 and PAN10). PAN10 is known for its tighter pore structure when compared with other commercial available UF membranes. Hence interfacial polymerization on such a membrane could result in an even lower permeate flux and a lower rejection when compared with that of PAN400.

In the main study, ionic liquids BMIC and OMIC were substituted for water in the interfacial polymerization process of 1% PIP. The resulting TFNC membranes made with this process were evaluated with MgSO_4 and NaCl for their salt rejection and flux. The results suggested that the molecular size and geometry of the IL could play a beneficial role in tailoring the performance of the barrier layer. For instance, TFNC membranes prepared with BMIC exhibited an overall improvement in salt rejection (i.e. MgSO_4 : 99.1 to 99.2% and NaCl : 37.3 to 58.8%) accompanied by a reduction in the permeate flux (i.e. 32.45 to 12.86 $\text{l/m}^2\text{h}$) when the concentration of BMIC increased from 0.0 to 2.5%. This trend exhibited by the membrane prepared with BMIC indicates that perhaps the barrier layer became thicker and denser, thereby increasing the salt rejection and resistance to permeate flow. This type of behavior portrayed by BMIC is similar to that of phase transfer catalysts that are mentioned in studies by other groups. In contrast, TFNC membranes prepared with OMIC demonstrated a significant increase in permeate flux (i.e. 32.45 to 60.32 $\text{l/m}^2\text{h}$) and a slight decrease in salt rejection (i.e. MgSO_4 : 99.1 to 91.9% and NaCl : 37.3 to 24.3%). Unlike BMIC, the hydrophobic tail of OMIC entitled it to behave like a surfactant, which increases the free space between the pores during the formation of the polyamide matrix.

A TFNC membrane prepared with a combination of lower PIP concentration (i.e. 0.5% (w/v)) and lower OMIC concentration (i.e. 0.1% (w/v)) gave rise to filtration

performance with an overall improvement of 40.8% increase in permeate flux and 0.7% decrease in salt rejection compared to TFNC membrane prepared with equivalent PIP concentration and no ion liquids. This surpassed the performances of the more commonly used nanofiltration membrane (i.e. NF-90) and paralleled to that of the high-end commercial nanofiltration membrane, NF270. (i.e. permeate flux 50.03 l/m²h and 97.5%). Such an improvement could be attributed to a thinner membrane and an increase in the average pore size, which lowered the hydraulic resistance and enhanced the water transport capability. Further studies on the application of ionic liquids with other forms of polymeric barriers could provide useful advantages in tailoring the performance of the selective barrier layer.

References

- [1] Bottino A, Capannelli G, Comite A, Ferrari F, Firpo R, Venzano S. Membrane technologies for water treatment and agroindustrial sectors. *C. R. Chimie X* (2008) 1-7.
- [2] R. Petersen, Composite reverse osmosis and nanofiltration membranes. *J. Membr. Sci.* 83 (1993) 81–150.
- [3] Wang X, Chen X, Yoon K, Fang, Hsiao B, Chu B. High Flux Filtration Medium Based on Nanofibrous Substrate with Hydrophilic Nano-composite Coating. *Environ. Sci. Technol.* *Environ. Sci. Technol.* 2005, 39, 7684-7691.
- [4] Tang Z, Wei J, Yung L, Ji B, Ma H, Qiu C, Yoon K, Wan F, Fang F, Hsiao B, Chu B. UV-cured poly(vinyl alcohol) ultrafiltration nanofibrous membrane based on electrospun nanofiber scaffolds. *J. Membr. Sci.* 328 (2009) 1–5.
- [5] Mariñas B, Selleck R. Reverse osmosis treatment of multicomponent electrolyte solutions, *J. Membr. Sci.* 72 (1992) 211-229.
- [6] Bowen W, Mukhtar H, Characterisation and prediction of separation performance of nanofiltration membranes. *J. Membr. Sci.* 112 (1996) 263–274.
- [7] Eriksson P. Nanofiltration extends the range of membrane filtration. *Environ. Prog.* 7 (2006) 58–62.
- [8] Schaep J, Bruggen B, Vandecasteele C, Wilms D. Influence of ion size and charge in nanofiltration. *Separation Purification Technol.* 14 (1998) 155–162.
- [9] A.I. Schäfer, A.G. Fane and T.D. Waite, *Nanofiltration: Principles and Application*, Elsevier, Amsterdam (2005).
- [10] Yang F, Zhang S, Yang D, Jian X. Preparation and characterization of polypiperazine amide/PPESK hollow fiber composite nanofiltration membrane. *J. Membr. Sci.* 301 (2007)

85–92.

[11] Yoon K, Hsiao B, Chu B. High flux nanofiltration membranes based on interfacially polymerized polyamide barrier layer on polyacrylonitrile nanofibrous scaffolds. *J. Membr. Sci.* 326 (2009) 484– 492.

[12] Zhang Y, Xiao C, Liu E, Du Q, Wang X, Yu H. Investigations on the structures and performances of a polypiperazine amide/polysulfone composite membrane. *Desalination* 191 (2006) 291-295.

[13] Verissimo S, Peinemann K, Bordado J. Influence of the diamine structure on the nanofiltration performance, surface morphology and surface charge of the composite polyamide membranes *J. Membr. Sci.* 279 (2006) 266-275.

[14] Gopal R, Kaur S, Ma Z, Chan C, Ramakrishna S, Scaffoldsuura T. Electrospun nanofibrous filtration membrane. *J. Membr Sci* 281 (2006) 581–586.

[15] Singh P, Joshi S, Trivedi J, Devmurari C, Rao A, Ghosh P, *J. Membr. Sci.* 278 (2006) 19-25.

[16] Agarwal S, Wendorff J, Greiner A. Use of electrospinning technique for biomedical applications. *Polymer* 49 (2008) 5603–5621.

[17] Rho K, Jeong L, Lee G, Seo B, Park Y, Hong S, Roh S, Cho J, Park W, Min B. Electrospinning of collagen nanofibers: Effects on the behavior of normal human keratinocytes and early-stage wound healing. *Bioscaffolderials* 27 (2006) 1452-1461.

[18] Yoshimoto H, Shin Y, Terai H, Vacanti J. A biodegradable nanofiber scaffold by electrospinning and its potential for bone tissue engineering. *Bioscaffolderials* 24 (2003) 2077–2082.

[19] Bruggen B, Everaert K, Wilms D, Vandecasteele C. Application of nanofiltration for

removal of pesticides, nitrate and hardness from ground water: rejection properties and economic evaluation, *J. Membr. Sci.* 193 (2001) 239–248.

[20] Gibson P, Gibson H, Rivin D. Transport properties of porous membranes based on electrospun nanofibers. *Colloids and Surfaces A: Physicochemical and Engineering Aspects* 187 – 188 (2001) 469 – 481

[21] Ulbricht M. Advanced functional polymer membranes. *Polymer* 47 (2006) 2217–2262

[22] Nyström M, Kaipia L, Luque S. Fouling and retention of nanofiltration membrane. *J. Membr Sci.* 98 (1995) 249-262.

[23] Gao H, Jiang T, Han B, Wang Y, Du J, Liu Z, Zhang J. Aqueous/ionic liquid interfacial polymerization for preparing polyaniline nanoparticles. *Polymer* 45 (2004) 3017–3019.

[24] Rogers R, Seddon K. Ionic liquids – solvents of the future? *Science* 302 5646 (2003) 792–793.

[25] Theron S, Zussman E, Yarin A. Experimental investigation of the governing parameters in the electrospinning of polymer solutions *Polymer* 45 (2004) 2017–2030

[26] Thompson C, Chase G, Yarin A, Reneker D. Effects of parameters on nanofiber diameter determined from electrospinning model. *Polymer* 48 (2007) p. 6913.

[27] <http://www.Sepromembranes.com/>.

[28] Phillip Gibson P, Gibson H, Rivin D. Transport properties of porous membranes based on electrospun nanofibers. *A Physicochem Eng Aspects* 187–188 (2001) 469-481.

[29] Harrisson S, Mackenzie S, Haddleton D. Pulsed Laser Polymerization in an Ionic Liquid: Strong Solvent Effects on Propagation and Termination of Methyl Methacrylate. *Macromolecules* 36 14 (2003) 5072–5075.

[30] Kuehne M, Song R, Li N, Peterson R. Flux enhancement in TFC RO membranes.

Environmental progress 20 (2001) 23-26.

[31] Zhang X, Chan-Yu-King R, Jose A, Manohar S. Nanofibers of polyaniline synthesized by interfacial polymerization. *Synthetic Metals* 145 (2004) 23–29

[32] Dallas P, Stamopoulos D, Boukos N, Tzitzios V, Niarchos D, Petridis D. Characterization, magnetic and transport properties of polyaniline synthesized through interfacial polymerization. *Polymer* 48 (2007)

[33] Rahimpour A, Madaeni S, Mansourpanah Y. The effect of anionic, non-ionic and cationic surfactants on morphology and performance of polyethersulfone ultrafiltration membranes for milk concentration. *Journal of Membrane Science* 296 (2007) 110–121

[34] Boyer B, Hambarzoumian A, J Rogue, N Beylerian. Reaction in Biphasic Water/Organic Solvent System in the Presence of Surfactant: Inverse Phase Transfer Catalysis versus Interfacial Catalysis *Tetrahedron* 56 (2000) 303–307

[35] Starks C. Phase-Transfer Catalysis. Heterogeneous Reactions Involving Anion Transfer by Quaternary Ammonium and Phosphonium Salts. *J. Am. Chem. Soc.* 1971, 93 (1) 195–199

[36] Mathias L, Vaidya R. Inverse Phase Transfer Catalysis. First Report of a New Class of Interfacial Reactions. *J. Am. Chem. Soc.* 1986, 108, 1093-1094

[37] Song Y, Patricia Sun P, Henry L, Sun B. Mechanisms of structure and performance controlled thin film composite membrane formation via interfacial polymerization process . *Journal of Membrane Science* 251 (2005) 67–79

[38] <http://www.dow.com/liquidseps/>.